

This is a postprint version of the following published document:

Soria-Verdugo, A., Morato-Godino, A., Garcia-Gutierrez, L. M. & Garcia-Hernando, N. (2017). Pyrolysis of sewage sludge in a fixed and a bubbling fluidized bed – Estimation and experimental validation of the pyrolysis time. *Energy Conversion and Management*, vol. 144, pp. 235–242.

DOI: [10.1016/j.enconman.2017.04.062](https://doi.org/10.1016/j.enconman.2017.04.062)

© 2017 Elsevier Ltd.



This work is licensed under a [Creative Commons Attribution-NonCommercial-NoDerivatives 4.0 International License](https://creativecommons.org/licenses/by-nc-nd/4.0/).

1 **Pyrolysis of sewage sludge in a fixed and a bubbling fluidized bed –**
2 **Estimation and experimental validation of the pyrolysis time**

3 Antonio Soria-Verdugo*, Andres Morato-Godino, Luis Miguel Garcia-Gutierrez,
4 Nestor Garcia-Hernando

5 *Carlos III University of Madrid (Spain), Energy Systems Engineering Group,*
6 *Thermal and Fluids Engineering Department. Avda. de la Universidad 30,*
7 *28911 Leganés (Madrid, Spain).*

8 * *corresponding author: asoria@ing.uc3m.es*

9 **Abstract**

10 Pyrolysis of sewage sludge was studied experimentally in a stainless-steel
11 reactor operated as a fixed or fluidized bed. A novel measuring technique,
12 consisting of measuring the mass of the whole reactor and the sample on a
13 scale, was applied. The scale was capable of measuring the whole mass of the
14 reactor with enough accuracy to detect the mass released by the sewage
15 sludge sample during its pyrolysis. This original measuring technique permitted
16 the measurement of the evolution over time of the mass of sewage sludge
17 supplied to the bed in batch during its pyrolysis while moving freely in the bed.
18 From the measurement of the mass of the solid residue remaining in the
19 reactor, the pyrolysis time of the sewage sludge sample can be obtained
20 accurately for each operating condition. Different operating conditions were
21 selected to analyze the evolution with time of the sample mass during the
22 pyrolysis process, including the bed temperature and the velocity of the
23 Nitrogen used as inert gas. An increase of the velocity of Nitrogen from that of a

24 fixed bed ($0.8U_{mf}$) to that of a low velocity bubbling fluidized bed ($2.5U_{mf}$)
25 accelerates remarkably the pyrolysis process, i.e. reduces the pyrolysis time,
26 however increasing the Nitrogen velocity further has a slight effect on the
27 characteristic velocity of the pyrolysis process. The pyrolysis process of sewage
28 sludge can also be accelerated by increasing the bed temperature, even though
29 the effect of the temperature is lower than that of the Nitrogen velocity.
30 Furthermore, a mathematical model based on a first order apparent kinetics for
31 the pyrolysis of sewage sludge was proposed. The model was employed to
32 estimate the pyrolysis time for each operating condition, obtaining a proper
33 agreement with the experimental measurements.

34 *Keywords:* Sewage sludge; pyrolysis; fixed bed; fluidized bed; pyrolysis time.

35 **Notation**

36 d_{bm} Particle diameter of the bed material [m].

37 d_i Inner diameter of the reactor [m].

38 d_p Particle diameter of sewage sludge [m].

39 g Gravity acceleration [$m\ s^{-2}$]

40 h Height of the reactor [m].

41 h_b Height of the fixed bed [m].

42 k Apparent rate constant [s^{-1}].

43 k_{500} Apparent rate constant for a reactor temperature of 500 °C [s^{-1}].

44 k_{600} Apparent rate constant for a reactor temperature of 600 °C [s^{-1}].

- 45 m Mass of the sample [kg].
- 46 m_0 Initial mass of the sample [kg].
- 47 m_{vol} Mass of volatiles remaining in the sample [kg].
- 48 m_{vol0} Initial mass of volatiles in the sample [kg].
- 49 m_{res} Mass of the solid residue in the sample [kg].
- 50 n Reaction order [-].
- 51 t Time [s].
- 52 t_{mod} Estimated pyrolysis time [s].
- 53 t_{pyr} Experimental pyrolysis time [s].
- 54 T Temperature [K].
- 55 T_{amb} Reference temperature [K].
- 56 U Gas velocity [m s^{-1}].
- 57 U_{mf} Minimum fluidization velocity [m s^{-1}].
- 58 V/V^* Reacted fraction [%].
- 59 X Percentage of mass of the sample [%].
- 60 X_{vol} Percentage of total volatile content [%].
- 61 X_{res} Percentage of solid residue [%].
- 62 ε_t Relative error of the pyrolysis time [%].
- 63 ε Void fraction of the bed material [-].

- 64 ρ_{bm} Particle density of the bed material [kg m^{-3}].
- 65 ρ_g Gas density at reactor temperature [kg m^{-3}].
- 66 $\rho_{g,amb}$ Gas density at reference temperature [kg m^{-3}].
- 67 μ_g Gas dynamic viscosity at reactor temperature [$\text{kg m}^{-1} \text{s}^{-1}$].
- 68 $\mu_{g,amb}$ Gas dynamic viscosity at reference temperature [$\text{kg m}^{-1} \text{s}^{-1}$].
- 69 ϕ Sphericity of the dense phase particles [-].

70 **1. Introduction**

71 Sewage sludge is the solid residue produced during the treatment of municipal
72 and industrial wastewater. The rapid development of urbanization and
73 industrialization has contributed to the dramatic increase of sewage sludge
74 production over the last decades [1], causing a critical problem of waste
75 management. The ways of disposing sewage sludge can be divided into three
76 main applications: landfill, agricultural use, and incineration or thermochemical
77 conversion [2]. Nonetheless, the European regulations limit the use of sewage
78 sludge for landfilling due to environmental problems, while the use for
79 agricultural purposes has been also restricted because of the harmful
80 components of sewage sludge such as heavy metals, polyaromatic
81 hydrocarbons, and polychlorinated biphenyls [3]. In contrast, sewage sludge
82 thermochemical conversion permits to recover energy, reduces the volume of
83 the residue by 70% and thermally destructs the pathogens [4].

84 Among the different thermochemical conversion processes, pyrolysis is
85 considered to be a promising sewage sludge disposal technology due to its

86 advantages, such as residue volume reduction, concentration of heavy metals,
87 and stabilization of waste [5]. Pyrolysis processes can be divided into
88 conventional or fast pyrolysis, depending mainly on the pyrolysis vapors
89 residence time in the reactor. In conventional pyrolysis, vapor residence times
90 can vary between 5 and 30 min, whereas in fast pyrolysis processes, typical
91 vapor residence times are around 1-5 s [6]. Fast pyrolysis of biomass is usually
92 employed for fuel liquid production because of the high yield of bio-oil generated
93 [7]. Even though fast pyrolysis of biomass has achieved a commercial status
94 [8], many aspects are still empirical, requiring further study to improve the
95 efficiency and reliability of the process, and the final product characteristics [9].

96 Despite the numerous studies published focusing on thermochemical
97 conversion of sewage sludge, most of them work with dry sludge due to the
98 significant reduction of the efficiency and the operating problems derived from
99 the conversion of wet sewage sludge. In this way, fluidized bed reactors permit
100 both the thermochemical conversion and the drying processes to be carried out
101 in the same reactor, avoiding a significant decrease in efficiency. Fluidized beds
102 are employed as industrial chemical reactors due to their ability to convert low
103 quality solid fuels, even wet sewage sludge, with a high efficiency and with an
104 associated low emission of pollutants. The homogeneous and low reaction
105 temperature of fluidized beds limits the emissions of NO_x , whereas sorbent bed
106 materials can be used for in-bed capture of SO_x emissions. The technology of
107 bubbling fluidized beds is adequate for the conversion of highly volatile fuels
108 such as biomass and organic waste, for which the conversion can occur in the
109 bubbling bed at low temperatures without the need of in-bed heat exchangers
110 [10]. The performance and emission level of bubbling fluidized beds are

111 influenced by fuel mixing [11], which can be improved by increasing the
112 fluidizing gas velocity [12-15].

113 The products obtained from the pyrolysis of biomass in a fluidized bed are
114 affected by the operating conditions, such as fuel particle diameter, pyrolysis
115 vapors residence time and reactor temperature. The bed temperature is
116 considered to be the most influential parameter and thus several authors have
117 focused their research on analyzing its effect on the liquid yield [16-18]. In these
118 works, the bed temperature that maximizes the liquid yield is studied. For low
119 reactor temperatures, the energy supplied to the fuel particles is limited and
120 thus the total amount of volatile matter is not released from the solid fuel. In
121 contrast, for high reactor temperatures, the pyrolysis vapors generated may
122 suffer secondary cracking reactions, resulting in an increase of non-
123 condensable gases, decreasing the liquid yield. Therefore, the optimal reactor
124 temperature to produce liquid fuel from a pyrolysis process is a moderate
125 temperature. Concerning the maximum bio-oil yield produced from the pyrolysis
126 of sewage sludge in fluidized bed reactors, Jaramillo-Arango et al. [19] obtained
127 a liquid production of 40 wt% for a temperature of 600 °C; the maximum liquid
128 yield reached by Alvarez et al. [20] was 48 wt% for a bed temperature of 500
129 °C; and Fonts et al. [21] reached a maximum liquid production of 40 wt% at a
130 temperature of 550 °C. Sun et al. [22] studied the pyrolysis of sewage sludge in
131 a wide range of temperatures between 300 and 900 °C, concluding that the
132 maximum liquid production from the condensation of the pyrolysis vapors was
133 obtained at moderate temperatures of around 550 °C. In fact, in a following
134 study [5], they focused the analysis of sewage sludge pyrolysis on a narrow
135 temperature range of 400-600 °C. Moreover, for temperatures above 650 °C the

136 char generated during the pyrolysis process may react with the water vapor
137 produced [23].

138 The secondary thermal cracking of the pyrolysis vapors depends also on their
139 residence time inside the reactor. To avoid the thermal cracking of the product
140 gas, which promotes the formation of non-condensable gases and diminishes
141 the formation of liquid yield, the residence time of the pyrolysis vapors at high
142 temperatures should be limited. The effect of this parameter on the bio-oil
143 production has been studied by several authors, showing an increase in the
144 liquid yield produced during the pyrolysis of sewage sludge when decreasing
145 the residence time [24, 25].

146 In this work, a novel measurement technique is employed to analyze the
147 evolution of the pyrolysis process of sewage sludge in a lab-scale bed reactor.
148 The reactor was installed over a precision scale capable of measuring the mass
149 released by the sewage sludge sample during its pyrolysis process, moving
150 freely inside the reactor. This original measurement technique permits the study
151 of the pyrolysis process to be focused on the solid fuel instead of analyzing only
152 the liquid and/or the gas produced. The measurement obtained from the scale
153 permitted the measurement of the evolution over time of the mass released by
154 the sample for various operating conditions. The pyrolysis of sewage sludge
155 was analyzed for six different Nitrogen velocities, from a velocity lower than the
156 minimum fluidization velocity, corresponding to a fixed bed, to a velocity three
157 times faster than the minimum fluidization velocity, which induces a bubbling
158 fluidized bed. For each gas velocity, two different bed temperatures, 500 °C and
159 600 °C, in the range for which the liquid fuel production from pyrolysis is
160 maximized, were tested. The pyrolysis time was obtained from the experimental

161 measurements, and a mathematical model based on a first order apparent
162 kinetics was proposed. The pyrolysis time estimated by the model was
163 compared to the experimental results obtaining a fairly good agreement.

164 **2. Theory**

165 Pyrolysis is a complex process in which a huge amount of chemical reactions
166 occur simultaneously or consecutively. The parallel reactions taking place are in
167 competition to each other and depend mainly on the pyrolysis conditions. A
168 simplified approach permits the variation of the sample mass with time, dm/dt ,
169 to be determined as a function of the remaining volatile matter in the sample,
170 m_{vol} , and an apparent rate constant, k , for a determined reaction order, n , [23]
171 as:

$$\frac{dm}{dt} = -k \cdot m_{vol}^n \quad (1)$$

172 The mass of the sample, m , at each time, t , can be determined as the
173 summation of the volatile matter remaining in the sample, m_{vol} , and the solid
174 residue, m_{res} .

$$m = m_{vol} + m_{res} \quad (2)$$

175 Considering a first order reaction, $n = 1$, which is the simplest and most
176 generally used case, the integration of Eq. (1) reads:

$$m = m_{vol0} \cdot \exp(-k \cdot t) + m_{res} \quad (3)$$

177 where m_{vol0} is the initial mass of volatiles in the sample. Dividing Eq. (3) by the
178 initial mass of the sample, m_0 , the evolution of the percentage of mass of the
179 sample, X , with time, t , can be estimated as a function of the initial percentage

180 of volatile content, X_{vol} , the percentage of solid residue, X_{res} , and the apparent
181 rate constant, k . Notice that the percentage of solid residue is related to the
182 initial volatile content of the sample as $X_{res} = 100 - X_{vol}$.

$$X = X_{vol} \cdot \exp(-k \cdot t) + X_{res} \quad (4)$$

183 3. Materials and methods

184 3.1. Experimental facility

185 The pyrolysis of the sewage sludge samples was carried out in a cylindrical lab-
186 scale fluidized bed reactor, made of stainless steel, with an inner diameter, d_i , of
187 4.7 cm and a height, h , of 50 cm. The heat required to reach the reactor
188 temperature for the pyrolysis was supplied by three electric resistors with a
189 power of 500 W each one; one of them was located at the plenum and the other
190 two over the distributor. A potentiometer was employed to control the thermal
191 power released by the resistors. Nitrogen was used as the inert fluidization gas.
192 The Nitrogen flowrate was supplied by a B50 bottle from Abelló Linde,
193 containing Nitrogen 3.0 at a pressure of 200 bar. The Nitrogen flowrate was
194 measured by a flowmeter PFM750-F01-F from SMC, with a measurement
195 range from 1 to 50 l/min. The whole reactor, surrounded by the three resistors,
196 rested on a precision scale PS 6000 R2 from RADWAG, capable of measuring
197 up to 6 kg with a resolution of 0.01 g. A schematic of the experimental facility
198 employed to conduct the pyrolysis experiments is shown in Fig. 1.

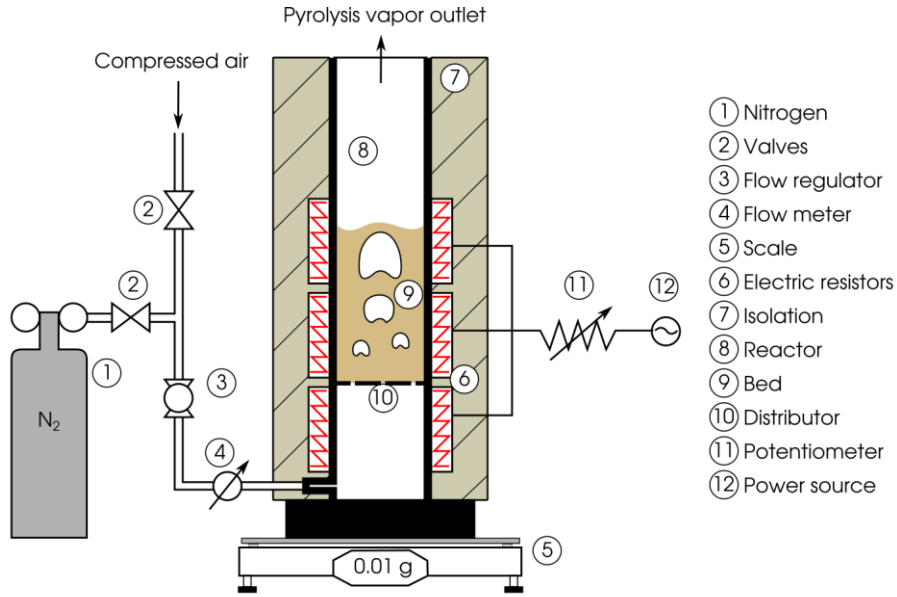


Fig. 1: Schematic of the experimental facility.

199
200

201 3.2. Bed material characterization

202 Silica sand was employed as bed material since it is known to be inert, not
 203 affecting the reaction rate during the thermochemical decomposition of biomass
 204 [26]. The silica sand particle diameter, d_{bm} , was in the range of 425 - 600 μm
 205 and the particle density, ρ_{bm} , was 2600 kg/m^3 . A mass of 240 g of sand was
 206 used in each test to reach a fixed bed height, h_b , of 9.4 cm (bed aspect ratio
 207 $h_b/d_i = 2$), corresponding to a void fraction, ε , of 0.44.

208 The variation of the gas density, ρ_g , with temperature was considered to
 209 determine the minimum fluidization velocity, U_{mf} , as described in Sánchez-
 210 Prieto et al. [27]. The gas density at the reactor temperature was calculated
 211 considering the ideal gas law:

$$\rho_g = \rho_{g,amb} \frac{T_{amb}}{T} \quad (5)$$

212 where ρ_g is the Nitrogen density at temperature T and $\rho_{g,amb}$ is the Nitrogen
 213 density at the reference temperature T_{amb} . The reference temperature was

214 selected as $T_{amb} = 300$ K and the Nitrogen density at this temperature is $\rho_{g,amb} =$
215 1.14 kg/m³.

216 The minimum fluidization velocity can be estimated as a function of the reactor
217 temperature using the correlation of Carman-Kozeny [28]:

$$U_{mf} = \frac{(\phi d_{bm})^2 (\rho_{bm} - \rho_g) g \varepsilon^3}{180 \mu_g (1 - \varepsilon)} \quad (6)$$

218 where U_{mf} is the minimum fluidization velocity, ϕ is the sphericity of the dense
219 phase particles, ε is the void fraction, g is the gravity acceleration, d_{bm} is the
220 diameter of the bed material particles, ρ_{bm} is the density of the bed material
221 particles, ρ_g is the density of Nitrogen at the reactor temperature, and μ_g is the
222 dynamic viscosity of Nitrogen at the bed temperature. The variation of the
223 dynamic viscosity of Nitrogen with the reactor temperature, T , can be
224 determined by the potential law:

$$\mu_g = \mu_{g,amb} \left(\frac{T}{T_{amb}} \right)^{2/3} \quad (7)$$

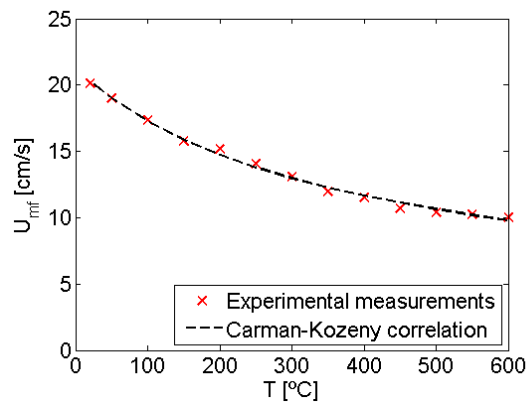
225 where the dynamic viscosity of Nitrogen at the reference temperature ($T_{amb} =$
226 300 K) is $\mu_{g,amb} = 1.78 \cdot 10^{-5}$ kg/(m·s).

227 **4. Results and discussion**

228 **4.1. Minimum fluidization velocity**

229 The minimum fluidization velocity of the silica sand particles was measured as a
230 function of the bed temperature. Fig. 2 shows the experimental results of the
231 minimum fluidization velocity, U_{mf} , together with the estimation from the
232 Carman-Kozeny correlation (Eq. 6), as a function of the reactor temperature, T .

233 An average particle diameter of silica sand of $d_{bm} = 512.5 \mu\text{m}$ and a sphericity
234 of $\phi = 0.8$ were selected for the Carman-Kozeny correlation. As can be seen in
235 Fig. 2, the estimation of the Carman-Kozeny correlation properly describes the
236 variation of the minimum fluidization velocity measured experimentally.



237
238 Fig. 2: Variation of the minimum fluidization velocity with the reactor
239 temperature.

240 4.2. Sewage sludge characterization

241 The sewage sludge samples employed in this work were produced by the
242 municipal sewage treatment plant of Loeches (Madrid, Spain) in February 2016.
243 The sludge was taken after a pre-drying process at 80 °C in a fluidized bed in
244 the sewage treatment plant. Proximate and ultimate analyses were performed
245 to characterize the samples. The former test was conducted in a TGA Q500
246 from TA Instruments, where the moisture, ash, volatile matter, and fixed carbon
247 contents of the sample were determined.

248 The ultimate analysis of the sample was carried out in a LECO TruSpec CHN
249 analyzer, where the Carbon and Hydrogen contents of the sample were
250 measured using an infrared absorption detector for the exhaust gases obtained
251 from the complete combustion of the sample carried out in pure Oxygen. The
252 Nitrogen content is determined conducting the exhaust gases through a thermal

253 conductivity cell. The results of the proximate and ultimate analyses of the
 254 sewage sludge samples are included in Table 1. Further details of the
 255 characterization of the sewage sludge samples can be found in Soria-Verdugo
 256 et al. [29]. The values obtained for the characterization of the sewage sludge
 257 are similar to those obtained by different authors, such as [30-33].

258 Table.1: Results obtained from the proximate and ultimate analyses of the
 259 sewage sludge (d: dry basis, daf: dry-ash-free basis, * obtained by difference).

Proximate analysis	
Volatile matter [% d]	57.11
Fixed carbon* [% d]	34.66
Ash [% d]	8.23
Elemental analysis	
C [% daf]	56.46
H [% daf]	7.91
N [% daf]	8.42
O* [% daf]	27.21

260 Prior to the pyrolysis experiments in the reactor, the sewage sludge samples
 261 were sieved under a particle size $d_p < 3$ mm and dried at 105 °C in a universal
 262 oven UFE 500 from Memmert for 5 hours, after which no mass variation of the
 263 sample was detected. The pyrolysis of this sewage sludge under linear,
 264 parabolic and exponential temperature increases in a thermogravimetric
 265 analyzer (TGA) was studied in detail in a previous work [29].

266 **4.3. Pyrolysis experimental measurements**

267 The sewage sludge pyrolysis experiments consisted of recording the mass
 268 signal measured by the scale while the pyrolysis process of the sewage sludge
 269 sample was taking place inside the reactor. Therefore, the mass released
 270 during the pyrolysis of the sampled could be determined. First, the reactor, filled
 271 with the sand particles that conformed the bed, was heated by the resistors to

272 the desired reactor temperature, T , while an air flowrate was used as fluidizing
273 agent. Once the reactor temperature of the test was reached, the fluidizing gas
274 was switched to Nitrogen, and the flowrate was adjusted. When the operating
275 conditions of the bed, i.e. reactor temperature and Nitrogen flowrate, were
276 selected, the scale, in which the reactor rested, was tared and a batch of
277 around 10 g of dry sewage sludge particles was introduced through the top of
278 the reactor. Each experimental measurement was replicated to test the
279 reproducibility of the experimental procedure, obtaining deviations lower than
280 5%.

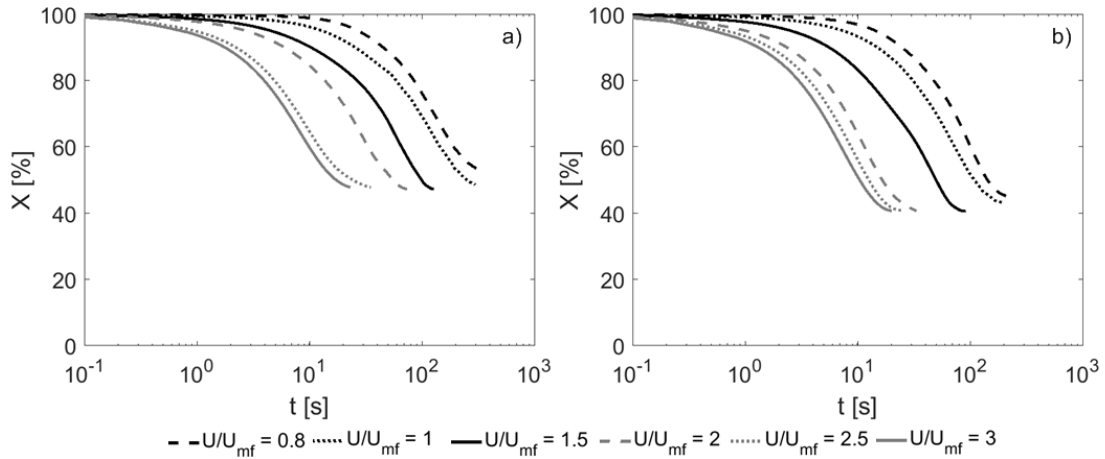
281 The mass signal measured by the scale during the pyrolysis of the sewage
282 sludge registered the vibration induced by the ascension of bubbles when the
283 bed was fluidized. Therefore, the mass signals measured in all cases were
284 filtered using a moving average. Further details of the filtration of the mass
285 signals can be found in a previous work [34]. The filtered signals were proved to
286 follow the average behavior of the raw signal measured by the scale in all
287 cases.

288 Different operating conditions were tested, varying both the reactor temperature
289 and the fluidizing gas velocity. The reactor temperatures analyzed in our work
290 are 500 and 600 °C, temperatures for which the production of liquid fuel from
291 the condensation of the sewage sludge pyrolysis vapors is optimal. A
292 thermogravimetric analysis of the pyrolysis of the same sewage sludge studied
293 in this work showed that most of the mass released by the samples during the
294 pyrolysis occurs for temperatures below 500 °C [29]. Concerning the velocity of
295 the fluidizing gas (Nitrogen) during the pyrolysis process, 6 different values
296 were tested for each reactor temperature, $U/U_{mf} = 0.8, 1, 1.5, 2, 2.5, 3$, from a

297 velocity lower than U_{mf} , corresponding to a fixed bed reactor, to 3 times U_{mf} ,
298 which induces a bubbling fluidized regime in the reactor. Gas velocities higher
299 than $3U_{mf}$ may produce large bubbles in the bed compared to the reactor
300 diameter, leading to a slugging regime, which is not the focus of this work.

301 **4.4. Evolution of the sewage sludge mass during the pyrolysis process**

302 The evolution with time of the mass of the sewage sludge sample during the
303 pyrolysis, measured by the scale, was filtered and divided by the initial mass of
304 the sample, m_0 , to obtain the percentage of mass remaining, X . The variation of
305 X with time during the pyrolysis of sewage sludge for each gas velocity
306 analyzed are plotted in Fig. 3 a) for a reactor temperature of 500 °C and in Fig.
307 3 b) for a bed temperature of 600 °C. The pyrolysis process is accelerated when
308 increasing the fluidizing gas velocity for the two reactor temperatures tested.
309 This fact can be attributed to the increase of the heating rate of the sewage
310 sludge particles [9, 35] caused by the higher axial fuel mixing obtained when the
311 fluidizing gas velocity is increased [14, 15]. Comparing the experimental
312 measurements obtained for both reactor temperatures, a slight effect of the
313 temperature can be observed, accelerating scarcely the pyrolysis process when
314 increasing the reactor temperature from 500 °C to 600 °C. Nevertheless, the
315 effect of the reactor temperature on the pyrolysis process is lower in
316 comparison with the significant effect of increasing the fluidization velocity.

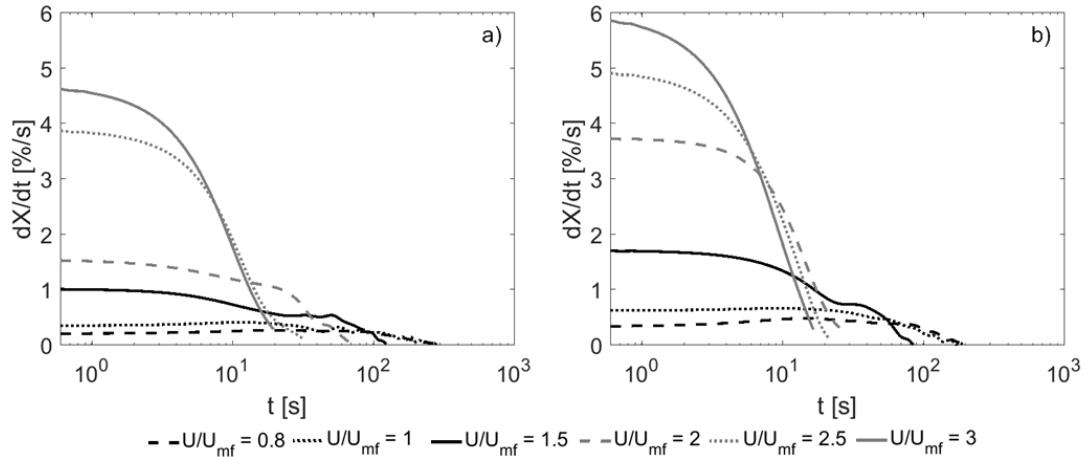


317
318

Fig. 3: Evolution with time of the percentage of mass of the sewage sludge

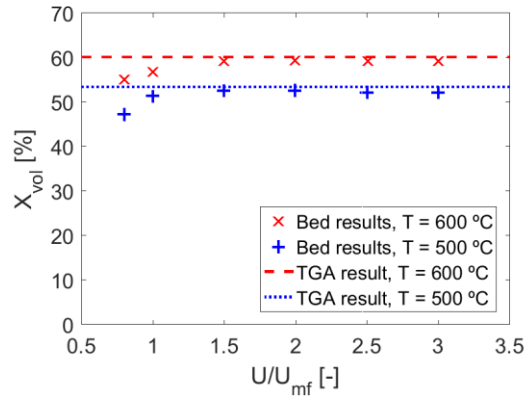
319 sample remaining in the reactor for a bed temperature of a) 500 °C and b) 600
320 °C.

321 To facilitate the analysis of the effect of the reactor temperature on the pyrolysis
322 process, the derivative of the percentage of mass remaining in the reactor is
323 plotted as a function of time in Fig. 4. The derivative of the percentage of mass
324 is clearly increased for both reactor temperatures when increasing the
325 fluidization velocity, accelerating the pyrolysis of the samples as stated above.
326 Comparing the results plotted in Fig. 4 a) for a reactor temperature of 500 °C
327 with those in Fig. 4 b) obtained for a bed temperature of 600 °C, the increase of
328 the derivative of X with temperature can be observed. Therefore, the pyrolysis
329 reaction of sewage sludge can be accelerated by increasing the gas velocity
330 and/or the reactor temperature.



331
 332 Fig. 4: Variation with time of the derivative of the percentage of mass of the
 333 sewage sludge sample remaining in the reactor for a bed temperature of a) 500
 334 °C and b) 600 °C.

335 The percentage of mass remaining after the pyrolysis process, X_{res} , can be
 336 determined as the percentage of mass at the end of the tests shown in Fig. 3. It
 337 can be observed in Fig. 3 that this percentage of mass remaining, X_{res} , depends
 338 on the operating conditions. To analyze the effect of both the reactor
 339 temperature and the Nitrogen velocity on the mass remaining after the
 340 pyrolysis, X_{res} , Fig. 5 shows the percentage of mass of volatiles released by the
 341 sample during the complete pyrolysis process, X_{vol} , defined as $X_{vol} = 100 - X_{res}$.
 342 Thermogravimetric analysis (TGA) tests of the pyrolysis of sewage sludge
 343 samples were also carried out for comparison to the pyrolysis tests in the
 344 reactor. The TGA tests were conducted in the TGA Q500 from TA Instruments
 345 and consisted of measuring the evolution of an initial mass of 10 mg of sewage
 346 sludge in a Nitrogen atmosphere at temperatures of 500 °C and 600 °C. The
 347 percentage of volatile matter released by the sewage sludge during the
 348 pyrolysis in the TGA is also included in Fig. 5 as dotted ($T = 500$ °C) and
 349 dashed ($T = 600$ °C) lines for comparison, although the Nitrogen flowrate for all
 350 the TGA tests was maintained constant at 60 ml/min.



351
352

Fig. 5: Total volatile matter released by the sewage sludge sample.

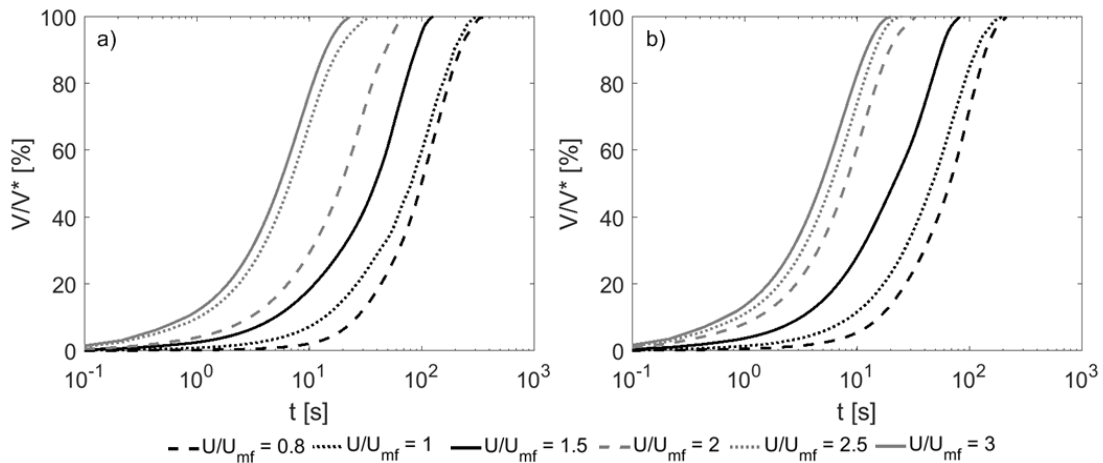
353 The percentage of volatile matter released by the samples during the pyrolysis
 354 process in the reactor is very similar to that obtained in the TGA, provided that
 355 the Nitrogen velocity is sufficient to induce a proper fluidization of the bed (U/U_{mf}
 356 ≥ 1.5). However, when the pyrolysis occurs in a fixed bed ($U/U_{mf} = 0.8$) or in a
 357 bed at minimum fluidization velocity ($U/U_{mf} = 1$), the value of X_{vol} obtained in the
 358 reactor is lower than that of the TGA. This can be attributed to heat transfer
 359 effects inside the sample when no bubbles are present in the bed ($U/U_{mf} \leq 1$)
 360 and the fuel particles accumulate on the bed surface after being introduced in a
 361 batch through the bed top, and thus the low conduction of heat inside this
 362 accumulation of fuel particles in the surface is important. When the gas velocity
 363 is increased above the minimum fluidization velocity ($U/U_{mf} > 1$), bubbles
 364 appear in the bed and induce the motion of fuel particles, breaking the typical
 365 accumulation of fuel found in fixed beds, and enhancing the axial dispersion of
 366 fuel inside the bed [14, 15]. Therefore, in the case of fluidized beds, the fuel
 367 particles are separated from each other due to the higher dispersion of fuel
 368 induced by the presence of bubbles, hence the effect of heat transfer inside the
 369 sample is reduced, and the heating rate is increased.

370 The values of the percentage of volatile matter released during the pyrolysis of
371 sewage sludge, X_{vol} , shown in Fig. 5 are in accordance with those reported by
372 different authors in the literature. Regarding the pyrolysis of sewage sludge in a
373 fixed bed, Wang et al. [1] obtained values of $X_{vol} = 50.9\%$ and $X_{vol} = 55\%$ for
374 reactor temperatures of 500 °C and 600 °C respectively, whereas Atienza-
375 Martínez et al. [36] reached $X_{vol} = 51\%$ for a bed temperature of 530 °C. Despite
376 the great heterogeneity in the composition of sewage sludge, these values are
377 quite close to those obtained in our work, $X_{vol} = 47.2\%$ for $T = 500$ °C and $X_{vol} =$
378 55.1% for $T = 600$ °C. Concerning the pyrolysis of sewage sludge in a fluidized
379 bed, Shen and Zhang [25] obtained percentages of volatile matter of $X_{vol} =$
380 55.2% and $X_{vol} = 57.4\%$ for fluidized bed temperatures of 500 °C and 600 °C,
381 respectively, which are comparable to those obtained in this work $X_{vol} = 53.4\%$
382 ($T = 500$ °C) and $X_{vol} = 60.1\%$ ($T = 600$ °C) in the TGA tests. Furthermore,
383 several authors informed of a reduction of the solid residue produced during the
384 pyrolysis of biomass for higher heating rates [9, 23, 37] and pyrolysis
385 temperatures [6, 16, 19, 20, 25].

386 **4.5. Pyrolysis time**

387 The effect of the different volatile matter released for each operating condition
388 can be removed by re-scaling the evolution of the percentage of sewage sludge
389 mass remaining in the reactor, X , shown in Fig. 3, to calculate the reacted
390 fraction, V/V^* . The reacted fraction, V/V^* , is defined as the ratio of the volatile
391 matter released at a determined time to the total volatile matter released after
392 the complete pyrolysis process, thus $V/V^* = 0\%$ at the beginning of the pyrolysis
393 process and $V/V^* = 100\%$ when the process ends. The results obtained for the
394 reacted fraction, V/V^* , are shown in Fig. 6, where a very similar shape of the

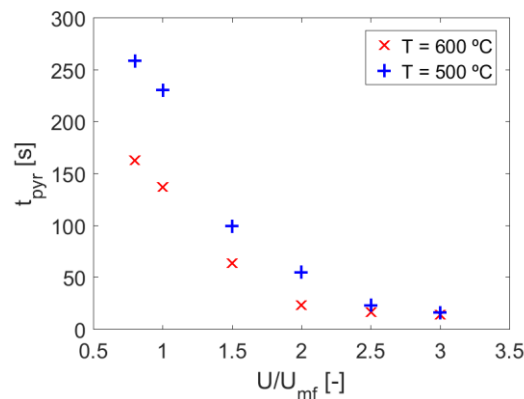
395 curves obtained for the different gas velocities and reactor temperatures can be
 396 observed. The increase of either the gas velocity or the bed temperature
 397 produces a displacement of the curves to shorter times, reducing the time
 398 needed for the pyrolysis of the sample.



399
 400 Fig. 6: Evolution of the reacted fraction of sewage sludge with time for reactor
 401 temperatures of a) 500 °C and b) 600 °C.

402 The pyrolysis time, t_{pyr} , can be calculated as the time needed to reach a
 403 determined value of the reacted fraction. In this work, a value of $V/V^* = 95\%$ is
 404 selected to determine the pyrolysis time. Fig. 7 shows the pyrolysis time of
 405 sewage sludge as a function of the Nitrogen velocity for the two different reactor
 406 temperatures studied. A substantial reduction of the pyrolysis time can be
 407 obtained by raising the fluidization velocity. The reduction of the pyrolysis time
 408 between a fixed or minimum fluidization bed ($U/U_{mf} \leq 1$) and a bubbling fluidized
 409 bed reactor ($U/U_{mf} \geq 1.5$) is significant, due to the higher heating rate
 410 characteristic of fluidized beds [24]. A clear reduction of the pyrolysis time with
 411 the reactor temperature can be also observed for low gas velocities ($U/U_{mf} <$
 412 2.5). However, these differences are negligible when increasing the Nitrogen
 413 velocity ($U/U_{mf} \geq 2.5$).

414 The reduction of the pyrolysis time produced by fluidized bed reactors is of
 415 central importance for industrial reactors since a lower pyrolysis time, i.e. faster
 416 pyrolysis reaction rate, permits the increase of the fuel feeding rate and, thus,
 417 the production of liquid fuel from the condensation of the pyrolysis vapors is
 418 enhanced. Furthermore, a higher fluidizing gas velocity reduces the pyrolysis
 419 vapors residence time in the reactor, promoting a higher content of condensable
 420 gases in the pyrolysis vapors, which further improves the production of liquid
 421 fuel from the pyrolysis of the sample [9, 17, 25].



422 Fig. 7: Pyrolysis time of sewage sludge for reactor temperatures of a) 500 °C
 423 and b) 600 °C.
 424

425 4.6. Modelling of the pyrolysis process of sewage sludge

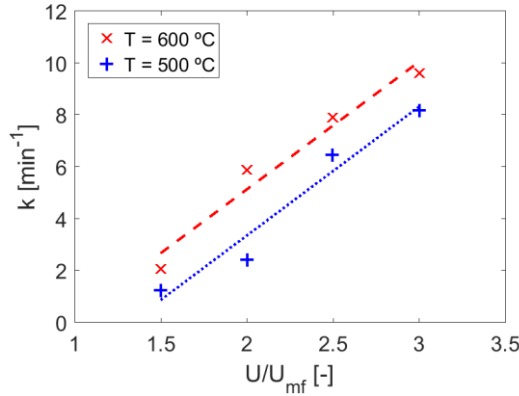
426 In this section, a mathematical procedure to estimate the pyrolysis time of
 427 sewage sludge as a function of the operating conditions of the reactor is
 428 presented. The procedure is based on determining the apparent rate constant,
 429 k , for the different gas velocities and reactor temperatures studied
 430 experimentally. The apparent rate constant, k , can be determined by fitting the
 431 experimental curves of the evolution of the percentage of mass of the sample,
 432 X , with time, shown in Fig. 3, to an exponential decay function in the form of Eq.
 433 (4). The fitting of the experimental curves $X - t$ was carried out only for Nitrogen

434 velocities high enough to properly fluidize the bed, i.e. $U/U_{mf} \geq 1.5$, causing a
 435 negligible effect of heat transfer inside the sample. For the pyrolysis tests of
 436 high gas velocities ($U/U_{mf} \geq 1.5$), the percentage of volatile matter released by
 437 the sewage sludge can be considered to be an exclusive function of
 438 temperature, being $X_{vol} = 53.4\%$ for a reactor temperature of 500 °C and $X_{vol} =$
 439 60.1% for a bed temperature of 600 °C (see Fig. 5). Therefore, the only free
 440 parameter on the fitting of the evolution of X with time to Eq. (4) is the apparent
 441 rate constant, k . The values obtained for the apparent rate constant, k , for each
 442 operating condition are included in Table 2, together with the determination
 443 coefficient, R^2 , of the fitting. As can be observed in Table 2, the determination
 444 coefficient, R^2 , is higher than 0.98 in all the cases analyzed, thus the
 445 experimental data of the variation of the percentage of mass of sewage sludge
 446 during the pyrolysis in the bubbling fluidized bed reactor can be said to follow a
 447 first order apparent kinetics.

448 Table 2: Values of the apparent rate constant and determination coefficient of
 449 the fitting for different gas velocities and reactor temperatures.

U/U_{mf} [-]	$T = 500$ °C		$T = 600$ °C	
	k [min^{-1}]	R^2 [-]	k [min^{-1}]	R^2 [-]
1.5	1.25	0.981	2.07	0.986
2	2.43	0.983	5.88	0.985
2.5	6.48	0.996	7.89	0.984
3	8.18	0.991	9.61	0.987

450 The values obtained for the apparent rate constant, included in Table 2, are
 451 depicted in Fig. 8 as a function of the dimensionless gas velocity, U/U_{mf} , for both
 452 reactor temperatures, along with a linear fitting of the data.



453
 454 Fig. 8: Apparent rate constant obtained from the fitting as a function of the gas
 455 velocity.

456 The variation of the apparent rate constant, k , with the dimensionless gas
 457 velocity, U/U_{mf} , was fitted to a linear equation, obtaining the slopes and
 458 intercepts presented in Eq. (8) and Eq. (9) for $T = 500$ °C and $T = 600$ °C,
 459 respectively. The increase of the apparent rate constant with the gas velocity is
 460 similar for the two reactor temperatures analyzed, as can be observed from the
 461 similar values of the slopes in Eqs. (8) and (9). The reactor temperature affects
 462 only the intercept of the linear fitting of the apparent rate constant with the
 463 dimensionless gas velocity.

$$k_{500} = 4.97(U/U_{mf}) - 6.59 \quad (8)$$

$$k_{600} = 4.92(U/U_{mf}) - 4.71 \quad (9)$$

464 The pyrolysis time can be estimated, t_{mod} , using the first order kinetic model
 465 described in section 2, as an only function of the apparent rate constant
 466 obtained for each bed temperature and gas velocity. Eqs. (8) and (9) can be
 467 used to estimate the value of the apparent rate constant for the pyrolysis of
 468 sewage sludge in a bubbling fluidized bed as a function of the gas velocity, for
 469 reactor temperatures of 500 °C and 600 °C, respectively. The estimated values

470 of the apparent reaction velocities, k_{500} and k_{600} , can be introduced in Eq. (4) to
 471 estimate numerically the evolution of the percentage of mass of the sewage
 472 sludge sample, X , with time during the pyrolysis process. This numerical
 473 estimation of the evolution of X with time can be rescaled to obtain a numerical
 474 reacted fraction, V/V^* , that can be employed to calculate the estimated pyrolysis
 475 time, t_{mod} , as the time for which the numerical reacted fraction reaches 95%.
 476 The results obtained for the estimation of the pyrolysis time, t_{mod} , are presented
 477 in Table 3 together with the experimental results, t_{pyr} , for comparison. The
 478 relative error, ε_t , between the estimated and the experimental pyrolysis time is
 479 also included in Table 3 for each operating condition of the fluidized bed
 480 reactor. The results presented in Table 3 show a good agreement between the
 481 prediction of the pyrolysis time by the model and the experimental results,
 482 obtaining relative errors around 10%.

483 Table 3: Comparison between the estimated and experimental pyrolysis times
 484 for different gas velocities and reactor temperatures.

$U/U_{mf} [-]$	T = 500 °C			T = 600 °C		
	t_{pyr} [s]	t_{mod} [s]	ε_t [%]	t_{pyr} [s]	t_{mod} [s]	ε_t [%]
1.5	99.9	111.2	11.3	63.7	60.9	4.4
2	55.6	49	11.9	23.7	26.3	11
2.5	23.4	25.8	10.2	17	19.1	12.3
3	16.8	17.5	4.2	14.3	14.9	4.3

485 5. Conclusions

486 The pyrolysis process of sewage sludge was studied experimentally in a bed
 487 reactor, analyzing the evolution of the sample mass with time for different
 488 reactor temperatures and gas velocities. For high gas velocities, corresponding
 489 to a bubbling fluidized bed regime ($1.5 \leq U/U_{mf} \leq 3$), the pyrolysis process was
 490 accelerated due to the higher heating rate of fuel particles in fluidized beds in

491 comparison to fixed bed reactors. The pyrolysis process occurs faster also for
492 higher reactor temperatures, although the effect of the bed temperature is slight
493 compared to that of the gas velocity. The percentage of volatile matter released
494 by the sewage sludge sample during the pyrolysis in a bubbling fluidized bed
495 reactor was around 53.4% for a bed temperature of 500 °C and 60.1% for a
496 temperature of 600 °C. These results are in accordance with the literature, and
497 very similar to those obtained from a thermogravimetric analysis of the samples.
498 The amount of volatile matter released by the sewage sludge is slightly lower
499 when the pyrolysis process is carried out in a fixed bed reactor.

500 The pyrolysis time was determined experimentally from the evolution of the
501 reacted fraction of the sewage sludge, showing an important diminution when
502 the gas velocity increases due to the larger heating rates characteristic of
503 bubbling fluidized beds. The effect of the reactor temperature is significant for
504 low gas velocities, whereas for high gas velocities the influence of the bed
505 temperature is negligible. A mathematical procedure, based on a first order
506 apparent chemical kinetics and capable of predicting the evolution of the
507 complex pyrolysis process, was proposed. The apparent pyrolysis rate constant
508 was obtained from a fitting of the experimental data to the first order kinetics
509 equation. The apparent rate constant showed a linear increase with the gas
510 velocity, maintaining a constant slope for the two different bed temperatures
511 studied. Finally, the mathematical model proposed was employed to estimate
512 the pyrolysis time for each operating condition, showing a good agreement with
513 the experimental pyrolysis time, obtaining deviations of around 10% for all the
514 operating conditions analyzed.

515 **Acknowledgments**

516 The authors gratefully acknowledge the financial support provided by Fundación
517 Iberdrola under the program “Programa de Ayudas a la Investigación en
518 Energía y Medioambiente”.

519 **References**

520 [1] Wang X., Deng S., Tan H., Adeosun A., Vujanovic M., Yang F., Duic N.
521 2016. Synergetic effect of sewage sludge and biomass co-pyrolysis: A
522 combined study in thermogravimetric analyzer and a fixed bed reactor. Energy
523 Conversion and Management 118, 399-405.

524 [2] Fonts I., Gea G., Azuara M., Ábrego J., Arauzo J. 2012. Sewage sludge
525 pyrolysis for liquid production: A review. Renewable and Sustainable Energy
526 Reviews 16, 2781-2805.

527 [3] Kaminsky W., Kummer A.B. 1989. Fluidized bed pyrolysis of digested
528 sewage sludge. Journal of Analytical and Applied Pyrolysis 16, 27-35.

529 [4] Fyttili D., Zabaniotou A. 2008. Utilization of sewage sludge in EU application
530 of old and new methods – A review. Renewable and Sustainable Energy
531 Reviews 12,116-40.

532 [5] Sun Y., Jin B, Wu W., Zuo W., Zhang Y., Zhang Y., Huang Y. 2015. Effects
533 of temperature and composite alumina on pyrolysis of sewage sludge. Journal
534 of Environmental Sciences 30, 1-8.

535 [6] Yan Q., Toghiani H., Yu F., Cai Z., Zhang J. 2011. Effects of pyrolysis
536 conditions on yield of bio-chars from pine chips. Forest Products Journal 61,
537 367-371.

- 538 [7] Bridgwater A.V. 2012. Review of fast pyrolysis of biomass and product
539 upgrading. *Biomass and Bioenergy* 38, 68-94.
- 540 [8] Bridgwater A.V., Peacocke G.V.C. 2000. Fast pyrolysis process for biomass.
541 *Renewable and Sustainable Energy Reviews* 4, 1-73.
- 542 [9] Bridgwater A.V., Meier D., Radlein D. 1999. An overview of fast pyrolysis of
543 biomass. *Organic Geochemistry* 30, 1479-1493.
- 544 [10] Leckner B. 2016. Developments in fluidized bed conversion of solid fuels.
545 *Thermal Science* 20, S1-S18.
- 546 [11] Leckner B. 1998. Fluidized bed combustion: Mixing and pollutant limitation.
547 *Progress in Energy Combustion Science* 24, 31-61.
- 548 [12] Soria-Verdugo A., García-Hernando N., Almendros-Ibáñez J.A., García-
549 Hernando U. 2011. Motion of a large object in a bubbling fluidized bed with a
550 rotating distributor. *Chemical Engineering and Processing* 50, 859-868.
- 551 [13] Soria-Verdugo A., García-Gutiérrez L.M., Sánchez-Delgado S., Ruiz-Rivas
552 U. 2011. Circulation of an object immersed in a bubbling fluidized bed.
553 *Chemical Engineering Science* 66, 78-87.
- 554 [14] Soria-Verdugo A., García-Gutiérrez L.M., García-Hernando N., Ruiz-Rivas
555 U. 2011. Buoyancy effects on objects moving in a bubbling fluidized bed.
556 *Chemical Engineering Science* 66, 2833-2841.
- 557 [15] Lundberg L., Soria-Verdugo A., Pallarès D., Johansson R, Thunman H.
558 2016. The role of fuel mixing on char conversion in a fluidized bed. *Powder*
559 *Technology*, In Press.

- 560 [16] Park E.S., Kang B.S, Kim J.S. 2008. Recovery of oils with high caloric
561 value and low contaminant content by pyrolysis of digested and dried sewage
562 sludge containing polymer flocculants. *Energy and Fuels* 22, 1335-1340.
- 563 [17] Park H.J., Heo H.S., Park Y.K., Yim J.H., Jeon J.K., Park J., Ryu C., Kim
564 S.S., 2010. Clean bio-oil production from fast pyrolysis of sewage sludge:
565 Effects of reaction conditions and metal oxide catalysts. *Bioresource*
566 *Technology* 101, 83-85.
- 567 [18] Arazo R.O., Genuino D.A.D., de Luna M.D.G., Capareda S.C. 2017. Bio-oil
568 production from dry sewage sludge by fast pyrolysis in an electrically-heated
569 fluidized bed reactor. *Sustainable Environmental Research* 27, 7-14.
- 570 [19] Jaramillo-Arango A., Fonts I., Chejne F., Arauzo J. 2016. Product
571 compositions from sewage sludge pyrolysis in a fluidized bed and correlations
572 with temperature. *Journal of Analytical and Applied Pyrolysis* 121, 287-296.
- 573 [20] Alvarez J., Amutio M., Lopez G., Barbarias I., Bilbao J., Olazar M. 2015.
574 Sewage sludge valorization by flash pyrolysis in a conical spouted bed reactor.
575 *Chemical Engineering Journal* 273, 173-183.
- 576 [21] Fonts I., Juan A., Gea G., Murillo M.B., Sánchez J.L. 2008. Sewage sludge
577 pyrolysis in fluidized bed, 1: Influence of operational conditions on the product
578 distribution. *Industrial & Engineering Chemistry Research* 47, 5376-5385.
- 579 [22] Sun Y., Jin B.S., Huang Y.J., Zuo W., Jia J.Q., Wang Y.Y. 2013.
580 Distribution and characteristics of products from pyrolysis of sewage sludge.
581 *Advanced Materials Research* 726, 2885-2893.

- 582 [23] Reschmeier R., Roveda D., Müller D., Karl J. 2014. Pyrolysis kinetics of
583 wood pellets in fluidized beds. *Journal of Analytical and Applied Pyrolysis* 108,
584 117-129.
- 585 [24] Piskorz J., Scott D.S., Westerberg I.B. 1986. Flash Pyrolysis of Sewage
586 Sludge. *Industrial & Engineering Chemistry Process Design and Development*
587 25, 265-270.
- 588 [25] Shen L., Zhang D.K., 2003. An experimental study of oil recovery from
589 sewage sludge by low-temperature pyrolysis in a fluidized-bed. *Fuel* 82, 465-
590 472.
- 591 [26] Koppatz M., Pfeifer C., Hofbauer H. 2011. Comparison of the performance
592 behavior of silica sand and olivine in a dual fluidized bed reactor system for
593 steam gasification of biomass as a pilot plant scale. *Chemical Engineering*
594 *Journal* 175, 468-483.
- 595 [27] Sánchez-Prieto J., Soria-Verdugo A., Briongos J.V., Santana D. 2014. The
596 effect of temperature on the distributor design in bubbling fluidized beds.
597 *Powder Technology* 261, 176–184.
- 598 [28] Carman P.C. 1937. Fluid flow through granular beds. *Transactions of the*
599 *Institute of Chemical Engineers* 15, 150-166.
- 600 [29] Soria-Verdugo A., Goos E., Morato-Godino A., Garcia-Hernando N., Riedel
601 U. 2017. Pyrolysis of biofuels of the future: Sewage sludge and microalgae –
602 Thermogravimetric analysis and modelling of the pyrolysis under different
603 temperature conditions. *Energy Conversion and Management* 138, 261-272.

- 604 [30] Scott S.A., Dennis J.S., Davidson J.F., Hayhurst A.N. 2006.
605 Thermogravimetric measurements of the kinetics of pyrolysis of dried sewage
606 sludge. *Fuel* 85, 1248-53.
- 607 [31] Soria-Verdugo A., Garcia-Hernando N., Garcia-Gutierrez L.M., Ruiz-Rivas
608 U. 2013. Analysis of biomass and sewage sludge devolatilization using the
609 distributed activation energy model. *Energy Conversion and Management* 65,
610 239-244.
- 611 [32] Jayaraman K., Gökalp I. 2015. Pyrolysis, combustion and gasification
612 characteristics of miscanthus and sewage sludge. *Energy Conversion and*
613 *Management* 89, 83-91.
- 614 [33] Liu G., Song H., Wua J. 2015. Thermogravimetric study and kinetic
615 analysis of dried industrial sludge pyrolysis. *Waste Management* 41, 128-133.
- 616 [34] Soria-Verdugo A., Morato-Godino A., Garcia-Gutierrez L.M., Garcia-
617 Hernando N. 2017. Pyrolysis of sewage sludge in a bubbling fluidized bed:
618 Determination of the reaction rate. 12th International Conference on Fluidized
619 Bed Technology (CFB 12). Krakow, Poland.
- 620 [35] Scott D.S., Piskorz J. 1984. The continuous flash pyrolysis of biomass.
621 *Canadian Journal of Chemical Engineering* 62, 404-412.
- 622 [36] Atienza-Martínez M., Fonts I., Lázaro L., Ceamanos J., Gea G. 2015. Fast
623 pyrolysis of torrefied sewage sludge in a fluidized bed reactor. *Chemical*
624 *Engineering Journal* 259, 467-480.
- 625 [37] Damartzis T.H., Vamvuka D., Sfakiotakis S., Zabaniotou A. 2011. Thermal
626 degradation studies and kinetic modeling of cardoon (*Cynara cardunculus*)

627 pyrolysis using thermogravimetric analysis (TGA). *Bioresource Technology* 102,
628 6230-6238.

629 **List of Figures**

630 Fig. 1: Schematic of the experimental facility.

631 Fig. 2: Variation of the minimum fluidization velocity with the reactor
632 temperature.

633 Fig. 3: Evolution with time of the percentage of mass of the sewage sludge
634 sample remaining in the reactor for a bed temperature of a) 500 °C and b) 600
635 °C.

636 Fig. 4: Variation with time of the derivative of the percentage of mass of the
637 sewage sludge sample remaining in the reactor for a bed temperature of a) 500
638 °C and b) 600 °C.

639 Fig. 5: Total volatile matter released by the sewage sludge sample.

640 Fig. 6: Evolution of the reacted fraction of sewage sludge with time for reactor
641 temperatures of a) 500 °C and b) 600 °C.

642 Fig. 7: Pyrolysis time of sewage sludge for reactor temperatures of a) 500 °C
643 and b) 600 °C.

644 Fig. 8: Apparent rate constant obtained from the fitting as a function of the gas
645 velocity.

646

647 **List of Tables**

648 Table.1: Results obtained from the proximate and ultimate analyses of the
649 sewage sludge (d: dry basis, daf: dry-ash-free basis, * obtained by difference).

650 Table 2: Values of the apparent rate constant and determination coefficient of
651 the fitting for different gas velocities and reactor temperatures.

652 Table 3: Comparison between the estimated and experimental pyrolysis times
653 for different gas velocities and reactor temperatures.